Composites Communications 31 (2022) 101107

Contents lists available at ScienceDirect

Composites Communications

journal homepage: www.elsevier.com/locate/coco

Multiple ply preforming of non-crimp fabrics with distributed magnetic clamping

Rajan Jagpal [a,b], Evangelos Evangelou [c], Richard Butler [a], Evripides G. Loukaides [a,b,*]

[a] Materials and Structures Research Centre, Department of Mechanical Engineering, University of Bath, BA2 7AY, Bath, United Kingdom
[b] Advanced Design and Manufacturing Centre, Department of Mechanical Engineering, University of Bath, BA2 7AY, Bath, United Kingdom
[c] Department of Mathematical Sciences, University of Bath, BA2 7AY, Bath, United Kingdom

ARTICLE INFO

Keywords:
Fabrics/textiles
Preforming
Laminate mechanics
Resin transfer moulding (RTM)

ABSTRACT

A major barrier to high-rate manufacture of non-crimp fabric (NCF) preforms is the relatively low volume of research evaluating multiple ply forming strategies. This study presents an extension to the distributed magnetic clamping (DIMAC) method towards establishing flexible process control measures for multiple ply forming. A measure of wrinkling was devised to allow comparison across different stack thicknesses and the distributions of wrinkles were shown to correlate with process parameters in an experimental parametric study. Further, ply-bending mechanics were shown to have a dominant effect on the draw-in of compression folds, particularly when increasing the number of equivalent biaxial plies. However, by deploying targeted distributed clamps, three-ply, single-stroke strategies over a complex positive curvature geometry became viable. DIMAC is shown to facilitate the local adjustment of boundary conditions whilst offering flexibility in improving component quality.

1. Introduction

High-rate automated resin transfer moulding (RTM) remains a challenge in the production of fabric composites. Non-crimp fabrics (NCF) in particular, due to complex material structure, represent the state-of-the-art in highly engineered materials. Manual processes still dominate production, with complex geometrical features representing challenges for automation. For example, automated tape lay-up (ATL) is hindered by minimum turning radii [1] and is only capable of intermediate geometrical complexity [2]. Drape forming has offered the most promise to date towards reduced cycle times and flexible tooling. However, drape forming processes offer little opportunity to control boundary conditions, greatly reducing the flexibility to influence the deformation and react to process-induced defects. What is more, composite forming processes can be highly variable which adds uncertainty and reduces the viability of machine learning and statistical inference towards process optimisation. Formability control approaches range from the addition of risers in double diaphragm forming (DDF) [3] to an operator manually pulling and relaxing the membrane over the tool in single diaphragm forming (SDF) protocols. These measures often further exacerbate variability. Continuous development of material systems and product geometries demand a solution that is highly repeatable, has adaptable process control measures, is translatable to different materials and offers process flexibility at different length scales. Despite the complexity of NCF materials, their architectures typically result in orthotropic properties and distinct energetically-favourable deformation modes. Hence, there is an opportunity to improve formability through tailored control during forming operations.

Approaches towards improving formability are available in the literature, both with *intrinsic* control (defined here as adjustments to the local in-plane stiffness through modifying the material itself [3–7]) and *extrinsic* controls (defined here as adjustments external to the material [8,9]). While intrinsic controls such as the resin overprinting and stitch removal offer promise, they remain difficult to implement on the shop floor. This is mainly due to the added processes that are inherent to any intrinsic method. By developing flexible extrinsic controls for material manipulation, pre-processing can be reduced. One robotic method is end-effector preform manipulation, which is fruitful at industrial scales [10], but requires expensive equipment and is relatively slow.

Most manufacturing processes still therefore rely on a ply-by-ply approach, which is time-consuming and resource-intensive, thus motivating industry to push towards the capability to lay down multiple ply stacks in one forming operation. Multiple ply forming of NCFs still remains a challenge with relatively little research in this area [5,11,12].

* Corresponding author. Materials and Structures Research Centre, Department of Mechanical Engineering, University of Bath, Bath, United Kingdom.
E-mail address: E.Loukaides@bath.ac.uk (E.G. Loukaides).

https://doi.org/10.1016/j.coco.2022.101107
Received 5 January 2022; Received in revised form 13 February 2022; Accepted 21 February 2022
Available online 23 February 2022

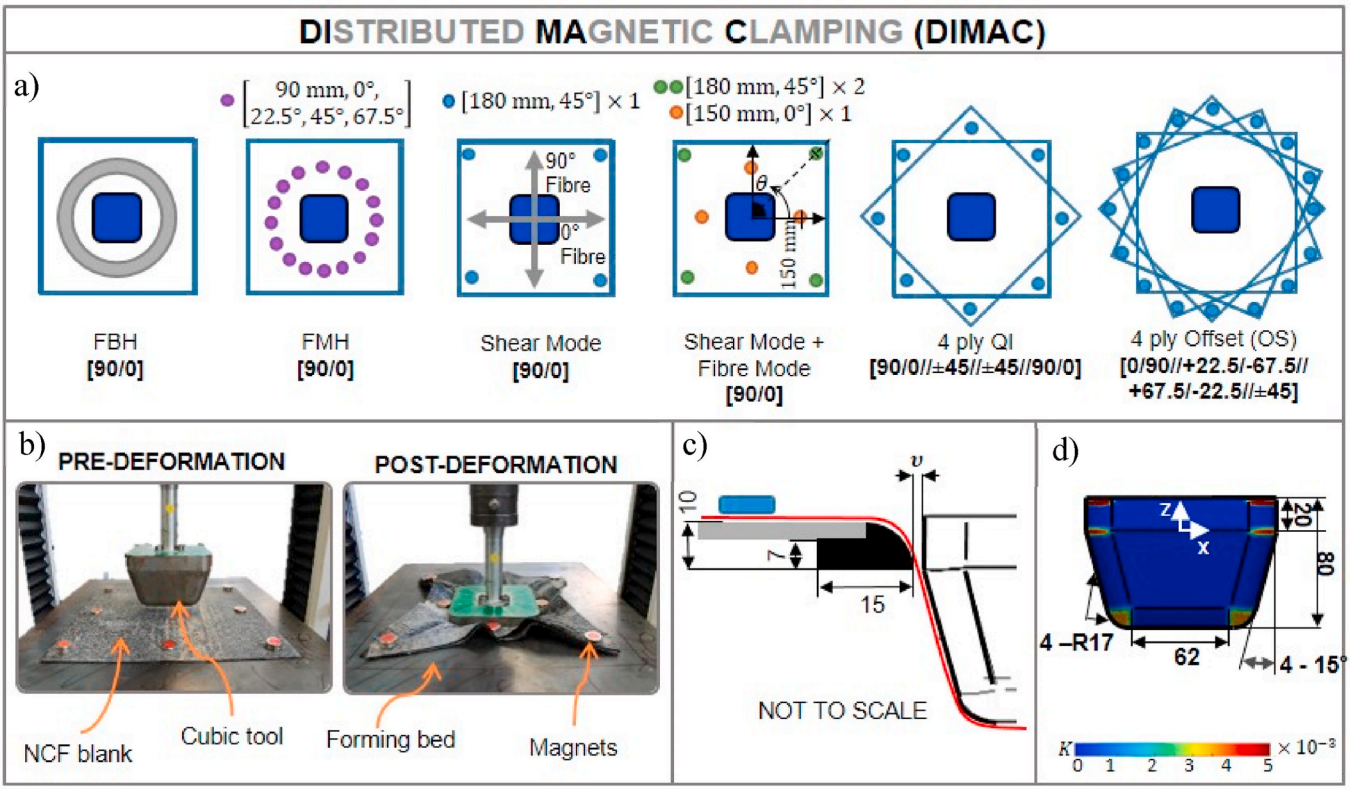

Fig. 1. a) The boundary conditions tested in this study with the coordinate systems origin at the centre of the tool and polar coordinate definition. b) Distributed magnetic clamping method showing the process pre- and post-deformation, c) cross section of the radial insert (black), forming bed (grey), magnet (blue) and deformed fabric (red) with material stack thickness indicated by υ, d) dimensions for the cubic geometry with overlaid Gaussian curvature, K. (For interpretation of the references to colour in this figure legend, the reader is referred to the Web version of this article.)

Interply friction is a key manufacturing barrier when aiming to increase stack size, due to the relatively high frictional anisotropy governing the complex surface interaction which can initiate wrinkling [7,11,12]. Contact effects however are often exacerbated when using process control measures that limit bending and force surface interactions - such as DDF, SDF and processes employing full circumferential blank holders. Reducing the constraints imposed on the material away from the target part, can facilitate out-of-plane deformation, which partly compensates for interply frictional effects.

Distributed magnetic clamping (DIMAC) was designed to work towards an automated, intelligent, RTM system. We previously gave details in Ref. [8] that highlighted its applicability in activating shear stretching modes to increase formability over single-ply forming scenarios. The process is similar to press forming but we replace a conventional blank holder with permanent magnets. These can be easily distributed across the surface of the sheet to affect boundary conditions and to influence local deformation mechanics. The intention is to improve component quality by preventing the emergence of wrinkles. However, to further validate DIMAC as a candidate for industrial development, increased understanding of single-stroke multiple ply forming is needed. Increasing the rate of production is antecedent to reducing the high cost of composite material part manufacture, allowing further added value not only to the aerospace and automotive sectors, but also to the national productivity strategy. In this paper, we use DIMAC to form multiple-ply stacks of NCF. We show the efficacy of increasing the number of plies formed in one operation and highlight some of the defect mechanisms that can be avoided through the addition of distributed magnetic clamps.

2. Method

2.1. Distributed magnetic clamping process for multiple ply forming

Experiments were performed utilising a veiled biaxial NCF (Tenax Teijen IMS65 E23 24K). This [90/v/0/v/pb] fabric had polyamide copolymer (CoPA) tricot-pillar stitches with interleaved chopped strand toughening veils (ET205). Powdered binder (EPIKOTE™ Resin 05311, 15 g m^{-2}) was applied to the outer veil by the manufacturer. The fibre (IMS65) elastic modulus was 290 GPa, with a measured fibre volume fraction of $V_f = 0.33$ for the NCF with a thickness of 1 mm. The remaining volume is taken up primarily by air but also by the non-structural elements such as the veil and stitches. For the purposes of this study, the front is defined as the 'fibre side' with stitches orthogonal to the 90° fibre and the back is defined as the 'veil side'. The DIMAC test apparatus was also adapted to facilitate multiple plies. This required six additional forming beds to accommodate material. The radial inserts took the geometry of the tools widest circumference on the xy plane, plus the nominal material thickness. This meant that for the NCF material studied here, 1 mm was added to each of the radial inserts central exclusion offset, from the tool perimeter, with each ply. The blank sizes used in all studies was 300 × 300 mm.

The NCF blank was placed on top (veil side up) of the forming bed and clamped in place using the magnets. The material was aligned with respect to x and y (Fig. 1), except for the offset (OS) and quasi-isotropic (QI) cases. In the OS test, each ply was spiral stacked undergoing a 22.5° rotation about z. In the QI example, the central two plies were instead both rotated 45° about z. Four magnetic clamps, per ply, were the minimum required to promote orthotropic in-plane shear deformation. We defined this arrangement with the coordinates [150 mm, $\theta + i90°$], where $i = 0, 1, 2, 3$. Polar coordinates [r, θ] are used to indicate the

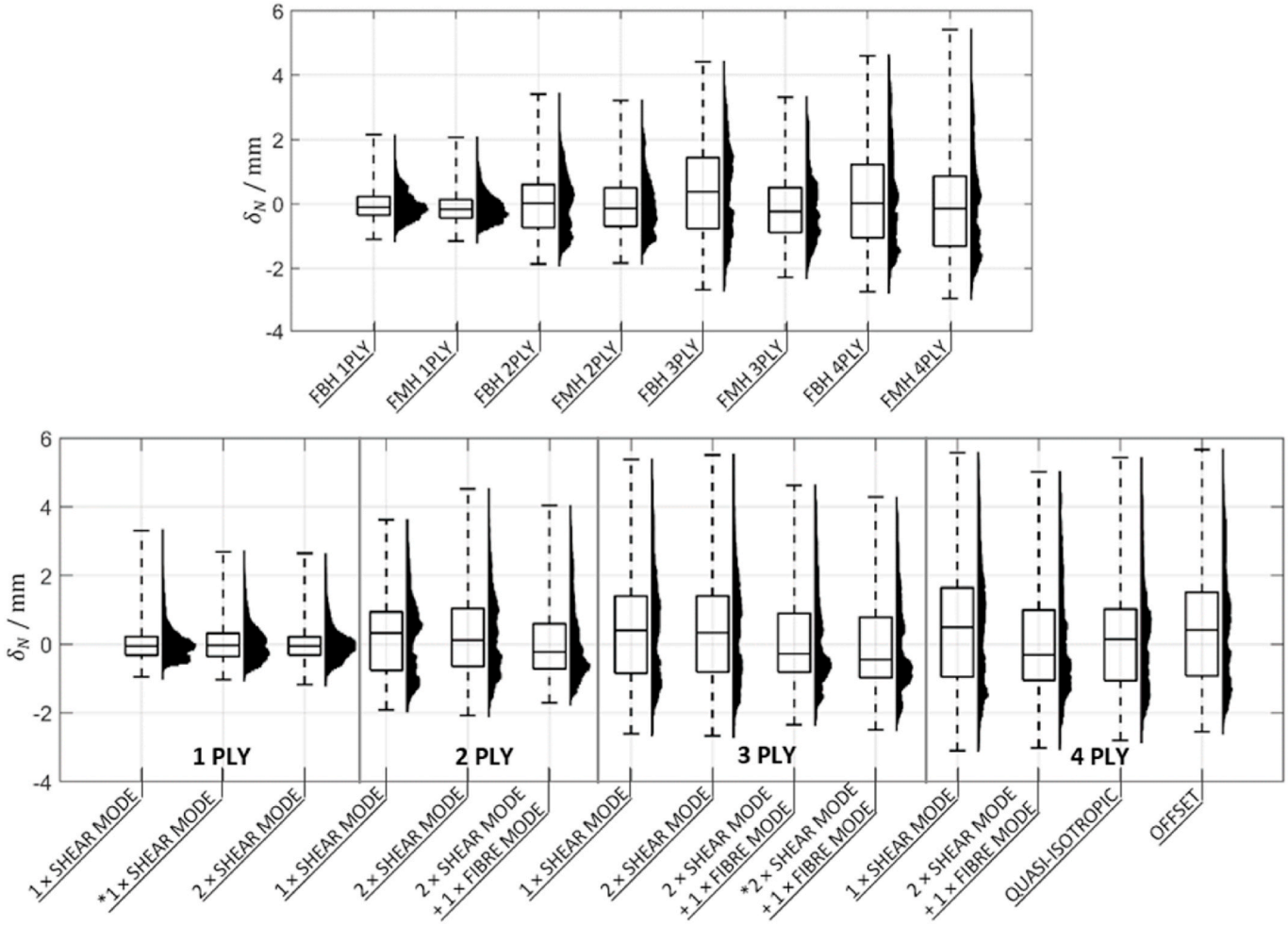

Fig. 2. Resulting histograms and boxplots of δ_N for all experiments showing the impact of boundary conditions to formability and material distribution. Repeated experiments indicated by * showing the low variance between metric statistics.

location of the magnets. As

Biaxial materials exhibit four key deformation modes [8], these were split into shear mode and fibre mode. Shear mode represents stretching at the midline between the NCFs fibre axis, through tow rotations about the pillar stitch. Fibre mode refers to boundary control along the fibre length. All fibre mode magnets were placed at radius 150 mm, with all shear mode magnets at 180 mm. Hence, a *shear mode* distribution of four magnets is given as [180, 45°], and a *fibre mode* distribution of four magnets as [150, 0°] for brevity. Further experiments doubled the magnetic clamping force by doubling the number of magnets at each location. To define these, a multiplication factor is indicated, hence a "2 × shear mode only" configuration indicates two magnets were stacked at each of the polar coordinates.

A further set of experiments was undertaken using a conventional full circumference blank holder (FBH) to reveal wrinkling differences with DIMAC. This was made from mild steel and had an annular geometry (2.13 kg, 180 mm inside-diameter, 198 mm outside-diameter, 48 mm depth). To facilitate comparison, experiments using a "full *magnet* holder" (FMH) were also conducted by placing 16 magnets as described in Fig. 1a at a radius of 90 mm. Permanent cylindrical magnets (N42) were employed in this study (diameter = 20 mm, thickness = 5 mm) with a clamping force of 90 N. In all cases the tool was lowered at a constant rate of 20 mm/min and began at the top of the material stack. This required stroke adjustment to accommodate the varying stack thicknesses and was calculated through the addition of the tool depth, radial insert depth and stack thickness, v.

2.2. Adjusted defect metric for multiple plies

Photogrammetry was used to capture the final surface and produce a representative point cloud. The process allowed comparison across different ply thicknesses, and utilised the software package CloudCompare [13], to increase computational efficiency. First the tool was re-meshed with target size of 1 mm. The distance of the outer surface of the material from the tool along the normal to the tool surface was calculated. Then the idealised ply thickness was subtracted from this distance. This calculation was performed at every node of the tools mesh and is represented by the metric δ_N. Positive values of indicate thickening or the emergence of wrinkles while negative values represent stretching and thinning of the material as it is pressed against the tool. Calculating δ_N at each point in the point cloud (~1 million points), also allows assessment of the defects spatial distribution.

3. Results and discussion

The distributions of δ_N for all experiments are shown in Fig. 2. The metric produced a comparable data-set with all medians close to 0. Analysis of these results is presented in three subsequent sections: *increasing the number of equivalent biaxial plies*, *increasing blank holder force (BHF)*, *varying magnet placement*, and finally *varying fibre angle*. First, the standard control method using a FBH revealed that by fully constraining the fabric in-plane, the median and maximum of δ_N were consistently higher than for the FMH cases up to three plies. For FMH at four plies, the maximum of δ_N was ~1 mm larger than for FBH, however

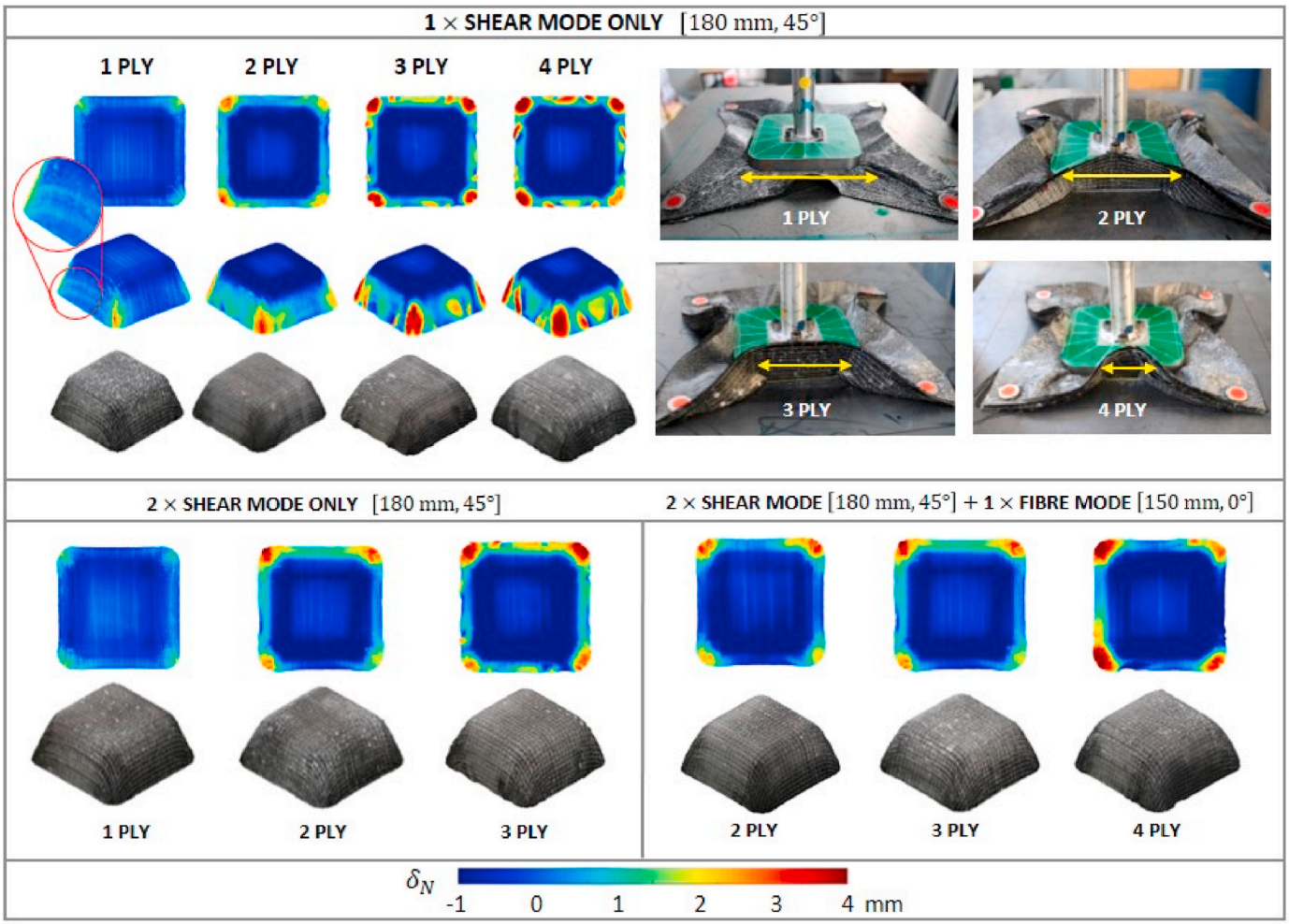

Fig. 3. Formed shapes for increasing number of biaxial plies with different boundary control parameters. Top surfaces of the "shear mode only" tests show the increasing stack stiffness with increasing plies and its impact on the evolution of bending between magnets and the draw-in point around the radial insert.

the median was still reduced. This reveals that the metric could distinguish some process-induced secondary deformation modes, such as fabric compaction, caused by tricot stitch deformation, fibre nesting, and the increased in-plane tension imparted by the magnets.

3.1. Increasing the number of biaxial plies

Initiating only shear mode boundary control led to the draw-in of large compression folds. A thickening was observed at the corners, caused by compaction of the fibre bundles. In the single ply trial, the shear thickening is seen in Fig. 3 ("1 × shear mode only"), where the curvature of the fibre path and subsequent increased thickness is highlighted by the magnified insert. As the number of plies increased, compression folds appeared at the lower portion of the corners and on the faces. Observing the top surfaces confirms that the coupling of plies raised the stiffness of the stack, something that is well understood by the increase in cross-sectional area. This increased stiffness, as well as increased interply shear, led to a draw-in of compression folds. Buckles on the faces evolved in magnitude with every additional ply. However, the experiment provided a basis from which to adapt boundary conditions in pursuit of high quality two or three ply forming.

3.2. Increasing blank holder force

An improvement to formability was found by increasing the BHF, which is consistent with other studies [14,15]. Doubling the clamping force has brought the median of δ_N, in every case, closer to zero - indicating reduced wrinkling. By examining the histograms in comparison with the "1 × shear mode" forming trials, a frequency reduction of larger δ_N values confirms this improvement. However, increasing the shear stress through doubling the magnet strength had no impact on the large compression folds that appeared at three plies and above.

3.3. Varying magnet placement and adapting boundary conditions

Detrimental compression folding and fabric buckling was addressed through additional "fibre mode" magnets. This added boundary condition ("1 × fibre mode") as well as the "2 × shear mode magnets", prevented the draw-in of defects on the faces. The hotspots on the corners (see Fig. 4) show that, even up to three plies formed in a single stroke, compression folding was reserved to the lower 10 mm. This leaves much of the geometry at three plies defect free. The histograms confirm that with all δ_N median results negative, most material adhered to the tool surface. The lengths of the positive tails have reduced and the range of δ_N is smaller. Adding the second boundary condition initiated fibre mode tension between each magnetic clamp and the material's areas of contact on the tool. This reduces the draw-in of the unconstrained material between clamps by increasing the in-plane tension. The fibre mode boundary condition also reduced the distance between each consecutive set of magnetic clamps. As the magnets slide in towards the tool, the fibre tow passing between the magnets must undergo compressive stress. Once this reaches a critical load, the fabric must buckle. However,

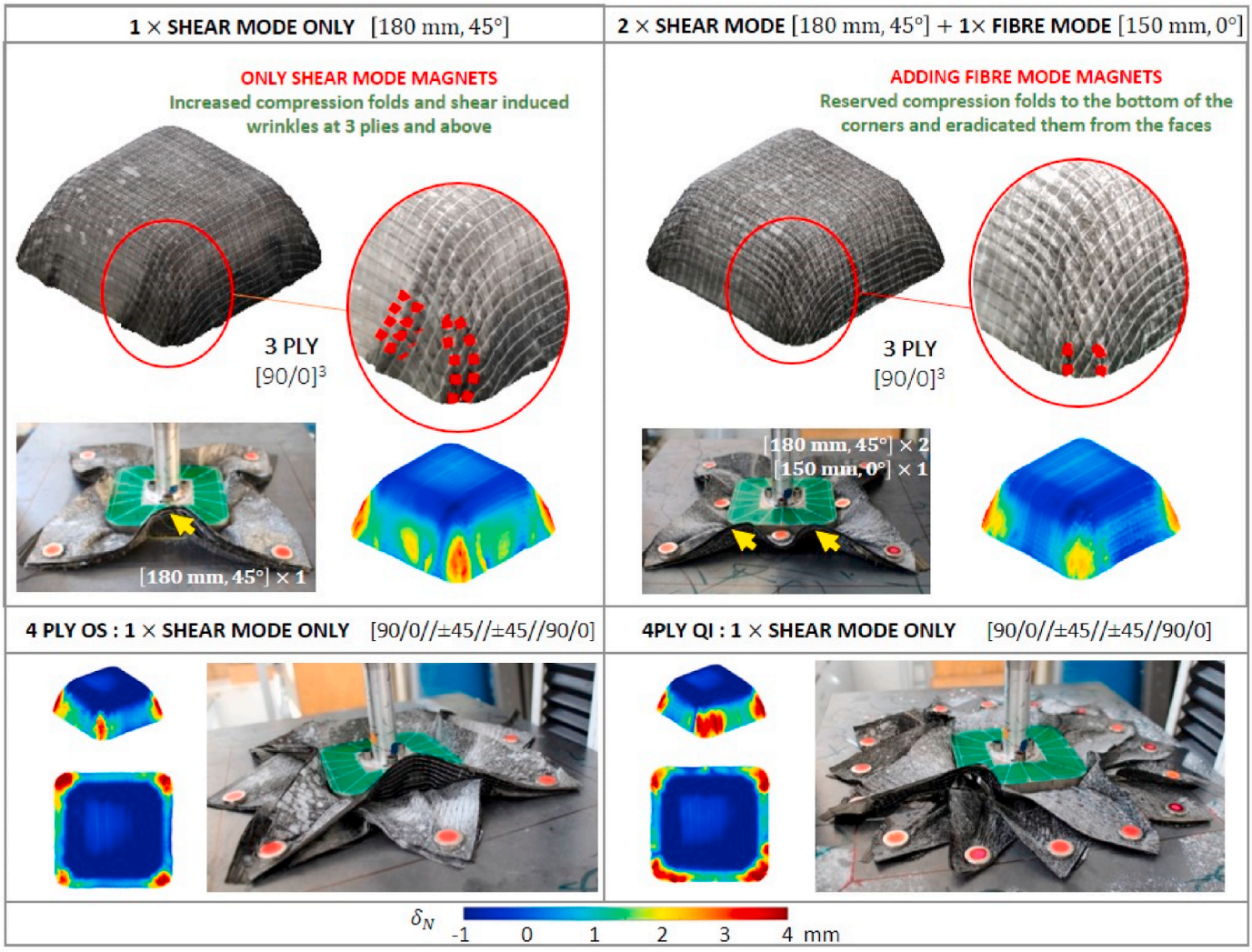

Fig. 4. Three ply example of the increase in formability and reduction in the draw-in of defects that can be attained through adding magnets and adapted boundary conditions. Four ply examples of varying fibre orientation are shown at the bottom.

by reducing this distance with the addition of another magnetic clamp, the critical load is increased. This reduced the effect of increased bending stiffness and produced two smaller amplitude buckles on the top surface while at the same time leading to a reduction in compression folding on the planar faces. This is highlighted in the three ply example in Fig. 4. Reduced wrinkling offers promise in optimising production, allowing the manufacture of complex geometries at multiple times the rate as previously possible.

3.4. Varying fibre orientation

From the two examples shown in Fig. 4, blank offsetting facilitated efficient arrangement of diverse fibre angles. Results further indicate that defects were primarily caused by compression folding. In the QI experiment, the ±45° plies are sandwiched between two [0°, 90°] NCF layers, resulting in the draw-in of large sub-surface compression folds at the radius. This effect is reduced in the OS test as none of the 4 plies are duplicated. Frictional coupling of the interply region is also increased in the QI example, with the relative angle between stitch and fibre increasing the contact area. This confirms that for complex geometrical features such as corners, fibre mode deformation does not allow adequate material shearing to conform to the geometry. However, the faces of the formed part are much better in the QI and OS examples than for four equivalent plies. Therefore, DIMAC is suitable for forming larger parts with more typical ply stacks, at a high rate. This includes aerospace parts such as large spars, secondary structures and panels.

4. Concluding remarks

Distributed magnetic clamping was shown to be a viable extrinsic control measure for multiple ply forming which reinforces the flexible nature of the platform. A measure of wrinkling correlated well with observed defects and allowed a composition between different ply stacks and boundary control arrangements. The outcomes of this work are summarised below:

- Increasing the number of biaxial plies formed in one stroke is possible by adapting the boundary conditions.
- Increasing the BHF by doubling the magnetic clamping force reduces shear induced wrinkling and brings our measure of wrinkling, δ_N, closer to zero in all cases.
- Moving to multiple plies increased the stack bending stiffness, particularly when there was a repetition of fibre angles. Using only shear mode magnets caused the draw-in of large macroscale wrinkles on the faces. Adding a second set of fibre mode magnets eradicated these wrinkles from the faces.
- Varying the fibre orientations of each biaxial ply within the stack while deploying tailored boundary control, showed potential to

influence individual ply deformation while still controlling the global deformation of the material stack.

Future work should include an exploration of the scalability of DIMAC to industrial size components and production environments. At the same time, the ability to locally influence formability for isolated features in a large part is potentially a powerful aspect of the process – including by clamping against the tool itself or changing the clamping during the forming process.

Declaration of competing interest

The authors declare that they have no known competing financial interests or personal relationships that could have appeared to influence the work reported in this paper.

Acknowledgements

Gratitude is extended to EPSRC and UKRI for supporting the work carried out under the National Productivity Investment Fund (NPIF) project (EP/R512424/1). Rajan Jagpal's PhD studentship is 50% funded by GKN Aerospace. The authors would like to particularly thank GKN Aerospace for providing industrial context and guidance. Prof. Richard Butler also holds the Royal Academy of Engineering - GKN Aerospace Research Chair.

References

[1] L.E. Culliford, C. Scarth, T. Maierhofer, R. Jagpal, A.T. Rhead, R. Butler, Discrete Stiffness Tailoring: optimised design and testing of minimum mass stiffened panels, Compos. B Eng. 221 (2021) 109026, https://doi.org/10.1016/j.compositesb.2021.109026.

[2] M. Di Francesco, C. Hopcraft, L. Veldenz, P. Giddings, Preforming large composite aerostructures: a unique UK capability, in: Paper Presented at SAMPE Europe Conference 2018, Southampton, United Kingdom, 2018.

[3] S. Chen, O.P.L. McGregor, L.T. Harper, A. Endruweit, N.A. Warrior, Optimisation of local in-plane constraining forces in double diaphragm forming, Compos. Struct. 201 (2018) 570–581, https://doi.org/10.1016/j.compstruct.2018.06.062.

[4] S. Chen, L.T. Harper, A. Endruweit, N.A. Warrior, Formability optimisation of fabric preforms by controlling material draw-in through in-plane constraints, Compos. Appl. Sci. Manuf. 76 (2015) 10–19, https://doi.org/10.1016/j.compositesa.2015.05.006.

[5] S. Chen, A. Endruweit, L.T. Harper, N.A. Warrior, Inter-ply stitching optimisation of highly drapeable multi-ply preforms, Compos. Appl. Sci. Manuf. 71 (2015) 144–156, https://doi.org/10.1016/j.compositesa.2015.01.016.

[6] Chen S, Harper LT, Endruweit A, Warrior NA. Optimisation of Forming Process for Highly Drapeable Fabrics. 20th International Conference on Composite Materials2015.

[7] F. Yu, S. Chen, L.T. Harper, N.A. Warrior, Double diaphragm forming simulation using a global-to-local modelling strategy for detailed defect detection in large structures, Compos. Appl. Sci. Manuf. 147 (2021) 106457, https://doi.org/10.1016/j.compositesa.2021.106457.

[8] R. Jagpal, R. Butler, E.G. Loukaides, Towards flexible and defect-free forming of composites through distributed clamping, Procedia CIRP 85 (2019) 341–346, https://doi.org/10.1016/j.procir.2019.09.008.

[9] F. Nosrat Nezami, T. Gereke, C. Cherif, Active forming manipulation of composite reinforcements for the suppression of forming defects, Compos. Appl. Sci. Manuf. 99 (2017) 94–101, https://doi.org/10.1016/j.compositesa.2017.04.011.

[10] S. Dutta, M. Körber, C. Frommel, Automated fixation of dry carbon fibre fabrics with RTM6 for autonomous draping and sensor-aided preforming, Procedia CIRP 85 (2019) 329–334, https://doi.org/10.1016/j.procir.2019.10.007.

[11] S. Allaoui, C. Cellard, G. Hivet, Effect of inter-ply sliding on the quality of multilayer interlock dry fabric preforms, Compos. Appl. Sci. Manuf. 68 (2015) 336–345, https://doi.org/10.1016/j.compositesa.2014.10.017.

[12] E. Guzman-Maldonado, P. Wang, N. Hamila, P. Boisse, Experimental and numerical analysis of wrinkling during forming of multi-layered textile composites, Compos. Struct. 208 (2019) 213–223, https://doi.org/10.1016/j.compstruct.2018.10.018.

[13] CloudCompare, v2.11.3 Anoia (2020) retrieved from http://www.cloudcompare.org/.

[14] J.S. Lee, S.J. Hong, W.-R. Yu, T.J. Kang, The effect of blank holder force on the stamp forming behavior of non-crimp fabric with a chain stitch, Compos. Sci. Technol. 67 (3) (2007) 357–366, https://doi.org/10.1016/j.compscitech.2006.09.009.

[15] W.-R. Yu, P. Harrison, A. Long, Finite element forming simulation for non-crimp fabrics using a non-orthogonal constitutive equation, Compos. Appl. Sci. Manuf. 36 (8) (2005) 1079–1093, https://doi.org/10.1016/j.compositesa.2005.01.007.